

# Transit timing variation in exoplanet WASP-3b<sup>\*</sup>

G. Maciejewski<sup>1,2,†</sup>, D. Dimitrov<sup>3</sup>, R. Neuhäuser<sup>1</sup>, A. Niedzielski<sup>2</sup>, St. Raetz<sup>1</sup>,  
Ch. Ginski<sup>1</sup>, Ch. Adam<sup>1</sup>, C. Marka<sup>1</sup>, M. Moualla<sup>1</sup> and M. Mugrauer<sup>1</sup>

<sup>1</sup>*Astrophysikalisches Institut und Universitäts-Sternwarte, Schillergässchen 2–3, D–07745 Jena, Germany*

<sup>2</sup>*Toruń Centre for Astronomy, N. Copernicus University, Gagarina 11, PL–87100 Toruń, Poland*

<sup>3</sup>*Institute of Astronomy, Bulgarian Academy of Sciences, 72 Tsarigradsko Chausse Blvd., 1784 Sofia, Bulgaria*

Accepted . Received ; in original form

## ABSTRACT

Photometric follow-ups of transiting exoplanets may lead to discoveries of additional, less massive bodies in extrasolar systems. This is possible by detecting and then analysing variations in transit timing of transiting exoplanets. We present photometric observations gathered in 2009 and 2010 for exoplanet WASP-3b during the dedicated transit-timing-variation campaign. The observed transit timing cannot be explained by a constant period but by a periodic variation in the observations minus calculations diagram. Simplified models assuming the existence of a perturbing planet in the system and reproducing the observed variations of timing residuals were identified by three-body simulations. We found that the configuration with the hypothetical second planet of the mass of  $\sim 15 M_{\oplus}$ , located close to the outer 2:1 mean motion resonance is the most likely scenario reproducing observed transit timing. We emphasize, however, that more observations are required to constrain better the parameters of the hypothetical second planet in WASP-3 system. For final interpretation not only transit timing but also photometric observations of the transit of the predicted second planet and the high precision radial-velocity data are needed.

**Key words:** planetary systems – stars: individual: WASP-3.

## 1 INTRODUCTION

The analysis of observations minus calculations ( $O - C$ ) diagrams is a great tool commonly used for astrophysical studies of eclipsing binaries or pulsating variables. This method has already brought discoveries of exoplanets. Variations in the  $O - C$  diagram of the pulsating subdwarf B HS 2201+2610 were interpreted as a fingerprint of a giant planet (Silvotti et al. 2007). More recently, two planets orbiting an eclipsing system HW Vir were announced by Lee et al. (2009) and Qian et al. (2010) found a giant planet around the hibernating cataclysmic binary system QS Vir. These discoveries are based on interpretation of the light-travel time effect generated by an additional body.

The timing of known transiting planets is also expected to lead to discovering additional planets (Miralda-Escudé 2002; Holman & Murray 2005; Agol et al.

2005; Steffen et al. 2007). In a single-planet extrasolar system a planet orbits its host star on a Keplerian orbit. If one assumes that the inclination of its orbit plane is close to  $90^\circ$ , transits occur at equal intervals. If there is another (not necessarily transiting) planet in the system it interacts gravitationally with the transiting planet and generates deviations from the strictly Keplerian case. These perturbations result in a quasi-periodic signal in an  $O - C$  diagram of the transiting planet. The transit timing variation (TTV) method can be sensitive to small perturbing masses in orbits near low-order mean-motion resonances (MMRs, Steffen et al. 2007). A terrestrial-mass planet perturbing a hot-Jupiter gas giant is expected to cause a TTV amplitude of  $\sim 1$  minute and this signal grows sharply as bodies approach a MMR (Steffen et al. 2007). One must note that deriving the orbital elements and mass of the perturber from TTV, however, is a difficult inverse problem (e.g. Nesvorný & Morbidelli 2008). For a given transiting planet the TTV signal depends on 7 unknown parameters of the perturbing planet, i.e. its mass, semi-major axis, eccentricity, inclination, nodal and periape longitudes and difference of mean orbital phases of both planets for a given epoch. Exploring such a 7-dimensional space of parameters is not a trivial task (Nesvorný & Beaugé 2010). The differ-

<sup>\*</sup> This work is based on observations made with the 60-cm telescope of the Rozhen National Astronomical Observatory, which is operated by the Institute of Astronomy, Bulgarian Academy of Sciences and the 90-cm telescope of the University Observatory Jena, which is operated by the Astrophysical Institute of the Friedrich Schiller University.  
<sup>†</sup> E-mail: gm@astro.uni-jena.de

**Table 1.** The summary of observing runs:  $X$  – the airmass range,  $N_{\text{exp}}$  – the number of useful exposures,  $T_{\text{exp}}$  – used exposure times,  $FWHM$  – the averaged full width at half maximum of a stellar profile. Dates are given at the beginning of nights.

Run	Date	Observatory	$X$	$N_{\text{exp}}$	$T_{\text{exp}}$ (s)	$FWHM$ (")
1	2009 July 28	Rozhen	1.01 – 1.29	283	30	1.5
2	2009 Aug. 21	Rozhen	1.04 – 1.92	200	60	1.5
3	2009 Sep. 03	Rozhen	1.01 – 1.38	298	30	1.3
4	2009 Sep. 27	Jena	1.05 – 1.94	797	8	3.2
5	2009 Nov. 03	Jena	1.13 – 2.32	531	10, 15	3.9
6	2010 Apr. 18	Jena	1.08 – 2.19	412	25, 30	4.8

ent configurations may generate similar TTV signals with the identical dominant periodicity (Ford & Holman 2007).

The timing effects have been already studied in several transiting planet system: TrES-1 (Steffen & Agol 2005; Rabus et al. 2009), HD 189733 (Miller–Ricci et al. 2008b; Hrudková et al. 2010), HD 209458 (Agol & Steffen 2007; Miller–Ricci et al. 2008a), GJ 436 (Bean & Seifahrt 2008), CoRoT-1 (Bean 2009), TrES-2 (Rabus et al. 2009), TrES-3 (Gibson et al. 2009), and HAT-P-3 (Gibson et al. 2010). In all these cases the authors could only put constraints on the parameters of a hypothetical second planet because no significant signals in  $O - C$  diagrams have been found so far. Díaz et al. (2008) announced detection of period variation in OGLE-TR-111b and suggested that it may be caused by a perturbing Earth-mass planet in an outer orbit. However, Adams et al. (2010) observed 6 new transits of OGLE-TR-111b and concluded that there is no compelling evidence for the timing variation in the system and placed an upper limit of about  $1 M_{\oplus}$  on the mass of a potential second planet in a 2:1 orbital resonance.

Our first efforts to detect TTV signal for the transiting planets XO-1b, TrES-1b and TrES-2b resulted in redetermining their transit ephemerides (Raetz et al. 2009a,b). In 2009 we launched an international observing campaign to detect and characterise a TTV signal in selected transiting exoplanets. The programme is realised by collecting data from 0.6–2.2-m telescopes spread worldwide at different longitudes. In this paper we present photometric observations obtained for transiting exoplanet WASP-3b.

The existence of a planet around the unevolved main sequence star WASP-3 ( $V = 10.485$  mag) was discovered by detecting transits followed by radial velocity measurements (Pollacco et al. 2008). The exoplanet turned out to be a strongly irradiated gas giant. Its mass and radius were found to be  $1.76_{-0.14}^{+0.08} M_J$  and  $1.31_{-0.14}^{+0.07} R_J$ , respectively. It orbits its host star in  $\sim 44$  h in a circular orbit with the semi-major axis of  $0.0317_{-0.0010}^{+0.0005}$  au. The orbital inclination was found to be  $84.4_{-0.8}^{+2.1}$  deg. The host star has a spectral type of F7–8V and photospheric temperature of  $6400 \pm 100$  K. Gibson et al. (2008) observed two transits with a photometric precision of  $\sim 4$  millimag (mmag) and redetermined the planetary radius  $1.29_{-0.12}^{+0.05} R_J$  and the orbital inclination  $85.06_{-0.15}^{+0.16}$  deg. The mean density of the planet was found to be  $0.82_{-0.09}^{+0.14} \rho_J$ . Moreover, Gibson et al. (2008) calculated new ephemeris which resulted in the orbital period of  $1.846835 \pm 0.000002$  d.

Simpson et al. (2010) presented a spectroscopic observation of the Rossiter–McLaughlin effect for WASP-3 system. The sky-projected angle between the stellar rotation

axis and planetary orbital axis  $\lambda$  was found to be  $15_{-9}^{+10}$  deg, i.e. consistent with zero within  $2\sigma$ . More recently, Tripathi et al. (2010) obtained spectra during two separate transits and got a more precise value  $\lambda = 3.3_{-4.4}^{+2.5}$  deg. These findings indicate that WASP-3b underwent relatively non-violent migration process which did not perturb it from the primordial alignment of the proto-planetary disk (Simpson et al. 2010). Furthermore, Tripathi et al. (2010) presented photometric observations of 6 transits, including one incomplete. Some deviations from the linear ephemeris were found and explained as a results of either genuine period variations or underestimating the transit time uncertainties. Tripathi et al. (2010) also redetermined planets’s mass which was found to be  $2.04 \pm 0.07 M_J$ .

The order of this paper is as follows. In Section 2 observations and data reduction are presented. The finding that the observed transit timing cannot be explained by a constant period is shown in Section 3. Preliminary configurations including a third body in the system (a perturbing planet), which may reproduce the observed variations of timing residuals, are identified and discussed in Section 4. Final conclusions are collected in Section 5.

## 2 OBSERVATIONS AND DATA REDUCTION

We observed 6 complete transits of WASP-3b with two telescopes both with the effective mirror diameter being 60 cm. While preparing observing runs only predicted complete transits during darkness were considered. Observations started  $\sim 1$  hour before the expected beginning of a transit and ended  $\sim 1$  hour after the event. Collecting long series of out-of-transit data is crucial in removing systematic trends and normalizing a light curve (e.g. Gibson et al. 2009; Hrudková et al. 2010). All observations were acquired in the R-band filter (Bessel 1990).

### 2.1 Rozhen

The CCD photometry of 3 transits on 2009 July 28, August 21 and September 3 was gathered with the 60-cm Cassegrain telescope at the Rozhen National Astronomical Observatory (NAO, Bulgaria), operated by the Institute of Astronomy, Bulgarian Academy of Sciences. The telescope was equipped with the CCD camera FLI PL09000 ( $3056 \times 3056$ ,  $12\mu\text{m}$  pixel). The field of view was  $17.3 \times 17.3$  with the scale of 0.334 arcsec per pixel. As a result of  $3 \times 3$  binning the final scale was 1.017 arcsec per pixel. Exposure times were selected on nightly basis to maximize the signal-to-noise (S/N)

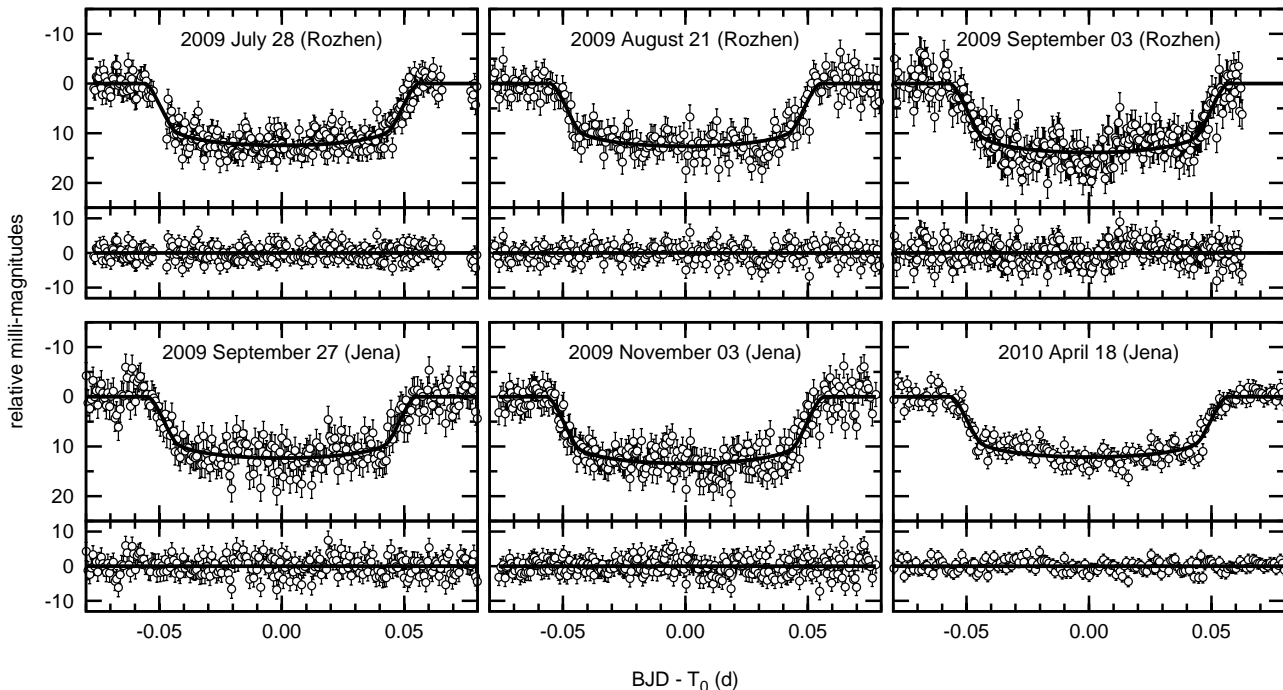


**Figure 1.** Light curves of WASP-3b transits in individual runs. The best-fitting models are shown as continuous lines. The residuals are presented in panels below each light curve.

ratio, keeping pixels unsaturated and intensity in the linear region of the CCD ( $<50000$  counts) for the object and probable standard stars.

The standard IDL procedures (adapted from DAOPHOT) were used for the reduction of the photometric data (dark frame subtraction and flat-fielding), and computing the differential aperture photometry. To measure instrumental magnitudes, we used apertures with radii of 3.2, 4, 5, 6, 7, 8 and 9 binned pixels and a background ring located between 12 and 16 pixels. The best precision was reached using an aperture of 4 binned pixels. Using the method of Everett & Howell (2001) several stars (4 to 6) with photometric precision better than 5 mmag were selected to create an artificial standard star used for differential photometry.

## 2.2 University Observatory Jena

Transits on 2009 September 27, November 3 and 2010 April 18 were monitored with the 90-cm reflector telescope at the University Observatory Jena. Observations were taken with the new CCD-imager STK (see Mugrauer & Berthold 2010) which was installed in the Schmidt-focus of the telescope ( $D = 60$  cm,  $f/D = 3$ ). The camera exhibits  $52'8 \times 52'8$  field of view with a pixel-scale of 1.546 arcsec per pixel. The exposure time was set to get the highest S/N ratio for the target and was adjusted during a run due to changes of the airmass and atmospheric transparency. During third run the telescope was significantly defocused and hence longer exposure times were used. Applying this method was expected to minimise random and flat-fielding errors (e.g. Southworth et al. 2009), as confirmed by our higher-quality light curve (see bottom right panel in Fig. 1).

CCD frames were processed using a standard procedure that included subtraction of a dark frame, flat-fielding with twilight flats, differential aperture photometry, and astrometric calibration with the software pipeline developed for the Semi-Automatic Variability Search sky survey (Niedzielski, Maciejewski & Czart 2003). The instrumental coordinates of stars in frames were transformed into equatorial ones making use of positions of stars brighter than  $V = 15.5$  mag and extracted from the Guide Star Catalogue. To measure instrumental magnitudes, we used apertures with radii of 5, 6, 7 and 8 pixels and a background ring located between 12 and 20 pixels. The 6 pixel aperture was found to produce light curves with the smallest scatter and they were used in further analysis. To generate an artificial comparison star, 30 per cent of the stars with the lowest light-curve scatter were selected iteratively from field stars not fainter than 3 magnitudes below the saturation level. To achieve the similar probing rate in all runs ( $\sim 1$  point per minute), 3 and 2 point binning of a final light curve was applied. The detailed summary of observing runs is presented in Table 1.

## 3 RESULTS

### 3.1 Light curve analysis

A model-fitting algorithm available via the Exoplanet Transit Database (Poddany, Brat & Pejcha 2010) was used to derive transit parameters: transit duration, depth and mid-transit time and their errors. The procedure employs the OCCULTSMALL routine of Mandel & Agol (2002) and the Levenberg–Marquardt non-linear least squares fitting algorithm. The latter routine also provides errors for the fitted

**Table 2.** Parameters of transit light-curve modelling.  $T_0$ ,  $T_d$ ,  $\delta$ ,  $\sigma$ , and  $E$  denote the mid-transit time, the transit time duration, the depth, the averaged standard deviation of the fit, and the epoch, respectively. The  $O - C$  values are given both in days and in errors of mid-transit times. Note that BJD times are based on Terrestrial Dynamic Time (TT).

Run	$T_0$ BJD - 2455000	$T_d$ (min)	$\delta$ (mmag)	$\sigma$ (mmag)	$E$	$O - C$ (d)	$O - C$ ( $T_0$ errors)
1	$41.41271 \pm 0.00049$	$161.0 \pm 1.6$	$12.4 \pm 0.3$	1.6	236	-0.00046	-0.9
2	$65.41995 \pm 0.00059$	$158.9 \pm 1.9$	$12.6 \pm 0.4$	1.9	249	-0.00207	-3.5
3	$78.34873 \pm 0.00058$	$163.7 \pm 1.9$	$13.9 \pm 0.5$	2.4	256	-0.00114	-2.0
4	$102.35933 \pm 0.00056$	$157.9 \pm 1.9$	$12.3 \pm 0.4$	2.1	269	+0.00120	+2.1
5	$139.29713 \pm 0.00049$	$162.9 \pm 1.6$	$13.4 \pm 0.4$	1.7	289	+0.00169	+3.4
6	$305.51082 \pm 0.00039$	$162.6 \pm 1.3$	$12.1 \pm 0.6$	1.2	379	+0.00018	+0.5

parameters (O. Pejcha 2010, private communication). Our tests showed that the errors of mid-transit times derived from Levenberg–Marquardt method are consistent within  $\pm 30$  per cent with these values obtained from a Markov Chain Monte Carlo algorithm. An impact parameter  $b = a \cos i / R_* = 0.448 \pm 0.014$ , where  $a$  is semi-major axis,  $i$  is inclination, and  $R_*$  is host-star radius, was taken from Gibson et al. (2008) and was fixed during the fitting procedure. The model-fitting algorithm uses the linear limb-darkening law, thus we used a linear limb-darkening law by Van Hamme (1993) with the linear limb-darkening coefficient linearly interpolated for the host star. To determine the zero-point shift of magnitudes and to remove systematic trends which may exist in our data, a first- or second-order polynomial was used. The mid-transit times were corrected from UTC to Terrestrial Dynamic Time (TT) and then transformed into BJD. Light curves with best-fitting models and residuals are shown in Fig. 1. Derived parameters are collected in Table 2.

We achieved an averaged photometric precision between 1.2 and 2.4 mmag. The mid-transit timing errors are in the range of 34–51 s. The mean transit duration was found to be  $161.2 \pm 2.3$  min – a value similar to  $159.8^{+1.3}_{-2.6}$  min reported by Pollacco et al. (2008) and noticeably smaller than  $165.2^{+1.2}_{-0.8}$  min reported by Gibson et al. (2008) and  $168.8 \pm 0.7$  min announced by Tripathi et al. (2010). The mean transit depth was found to be  $12.8 \pm 0.7$  mmag which results in a planet-to-star radii ratio  $\rho = 0.108 \pm 0.003$ . This value is within the range of planet-to-star radii ratios determined for individual transits by Tripathi et al. (2010). Pollacco et al. (2008) and Gibson et al. (2008) obtained smaller values, i.e.  $\rho = 0.1030^{+0.0010}_{-0.0015}$  and  $\rho = 0.1014^{+0.0010}_{-0.0008}$ , respectively.

### 3.2 Transit ephemeris

Having a long time span of observations we determined a new ephemeris. As a result of fitting a linear function of epoch and period  $P$ , we obtained:

$$T_0 = 2454605.56000 \pm 0.00011 \text{ (BJD, based on TT)}$$

$$P = 1.8468355 \pm 0.0000007 \text{ d.}$$

Individual mid-transit errors were taken as weights.

The  $O - C$  diagram was generated using the new ephemeris. The timing residuals are collected in Table 2. The  $O - C$  diagram is plotted in Fig. 2 where besides transit times reported in this paper the literature data are also shown. Fol-

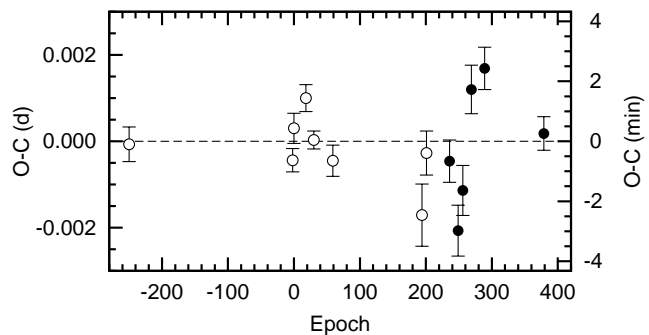


**Figure 2.** The observed minus calculated diagram for WASP-3b. The open symbols denote literature data (complete transits only) taken from Pollacco et al. (2008), Gibson et al. (2008) and Tripathi et al. (2010) while the filled ones denote results reported in this paper. Timing residuals were calculated using a new ephemeris derived in this study.

lowing Adams et al. (2010) we have confirmed that the times published by Pollacco et al. (2008), Gibson et al. (2008) and Tripathi et al. (2010) do not account for the UTC–TT correction (D. Pollacco 2010, private communication; A. Tripathi, private communication). Therefore, we added appropriate corrections to published times before analysing the  $O - C$  diagram. In the case of 3 points (1 from Tripathi et al. 2010 and 2 reported in this paper) timing residuals have a significance greater than  $3\sigma$ . That indicates that the uncertainties are underestimated or that the orbital period is not constant.

It is worth mentioning that data points from Rozhen lie below or close to zero level in the  $O - C$  diagram while those from Jena lie above it. This finding could suggest the presence of the systematic offset between both telescopes. However, our experience shows that this scenario seems to be unlikely. Simultaneous observations collected by both telescopes for another transiting planet gave difference between mid-transit times of 10 s only – much less than the error bars (Maciejewski et al. 2010, in prep.). One must note that error underestimating cannot be completely ruled out in our determinations but it would have a negligible influence on data point distribution and final conclusions.

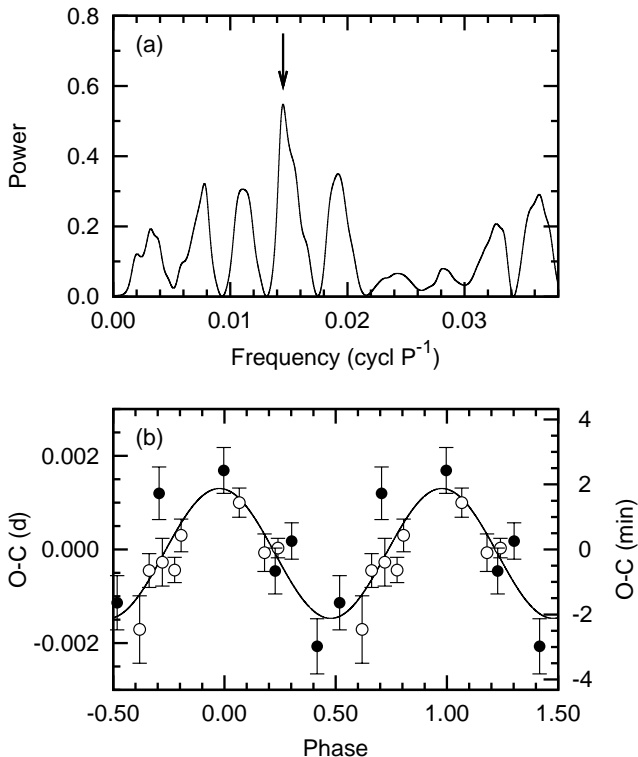


**Figure 3.** (a) A periodogram generated for timing residuals plotted in Fig 2, showing a peak at  $f_{\text{ttv}} = 0.0145 \text{ cycl } P^{-1}$ . (b) The  $O - C$  diagram phased with  $P_{\text{ttv}} = 69.0 \pm 2.4 P$  corresponding to  $f_{\text{ttv}}$ . The open and filled symbols denote literature and this paper (see Table 2) data, respectively. Note that data points were duplicated to cover phases from  $-0.5$  to  $1.5$ .

### 3.3 Search for a cyclic TTV

The timing residuals were searched for cyclic transit time variation by means of the analysis of variance method (ANOVA, Schwarzenberg-Czerny 1996) to identify any significant periodicities. Fig. 3a presents the generated periodogram covering frequencies  $f$  in the range of  $0.000$ – $0.038 \text{ cycl } P^{-1}$  where the upper limit is the calculated Nyquist frequency  $f_N$ . A significant peak was found around  $f_{\text{ttv}} = 0.0145 \text{ cycl } P^{-1}$  which corresponds to a period of  $P_{\text{ttv}} = 69.0 \pm 2.4 P$ . The  $O - C$  diagram phase-folded at  $P_{\text{ttv}}$  is plotted in Fig. 3b where the best-fitting sinusoid is also sketched. The semi-amplitude of variation was found to be  $0.0014 \pm 0.0002 \text{ d}$ .

## 4 DISCUSSION

### 4.1 Exomoon

A sinusoidal TTV might be caused by an exomoon around the transiting planet (Simon, Szatmáry & Szabó 2007; Kipping 2009). Kipping (2009) predicts that an exomoon also produces transit duration variation (TDV) with the same period as TTV and shifted by  $\pi/2$  in phase. That effect is not visible in TDV of WASP-3b. If the hypothetical moon is located at a Hill radius away from the planet, its mass is expected to be 6 per cent of the planetary mass to produce the observed TTV amplitude. This extreme value is

a lower limit of the mass because the needed mass increases as the moon is closer to the planet. Both tests indicate that the exomoon hypothesis is unlikely here.

### 4.2 Reanalysis of the radial velocity data

The possible non-zero eccentricity of the transiting planet may be a result of confusion with a two-planet system in which both planets orbit its host star in circular orbits and stay in an inner 2:1 resonance (Anglada-Escude et al. 2010). This degeneracy is a consequence of the Fourier expansion of the Kepler equation into powers of eccentricity. The non-zero eccentricity of the transiting planet may also betray the presence of an outer perturber in the system (see e.g. Fabrycky 2009). Tidal interactions with the star are expected to circularise the orbit of the transiting planet (Zahn 1977) but the presence of the second planet in the wider orbit may significantly delay this process (Mardling 2007).

The eccentricity of WASP-3b was reported to be statistically indistinguishable from zero. Pollacco et al. (2008) obtained  $e = 0.05 \pm 0.05$  and Simpson et al. (2010) got  $e = 0.07 \pm 0.08$ . Authors of both papers adopted  $e = 0.0$  in their analysis. Tripathi et al. (2010) adopted a priori circular orbit. We reanalysed the joined radial velocity data sets from Pollacco et al. (2008) and Tripathi et al. (2010) (only out-of-transit measurements) to test solutions with WASP-3b orbiting in an eccentric orbit. We used the SYSTEMIC CONSOLE software (Meschiari et al. 2009). The zero eccentricity Keplerian fit gives a reduced  $\chi^2 = 3.3$  with  $rms = 15.4 \text{ m s}^{-1}$ . If the eccentricity  $e$  is set as a free parameter the best-fitting model results in  $e = 0.05 \pm 0.04$  with a lower reduced  $\chi^2 = 2.3$  and  $rms = 13.9 \text{ m s}^{-1}$ . Our results show that the orbit of WASP-3b may be circular within  $2\sigma$  and the eccentric orbit cannot be excluded. The remaining dispersion of the radial velocity is typical for fast rotating late-type F stars (Saar, Butler & Marcy 1998).

### 4.3 Inner perturber

The mass of the perturbing planet in an inner 2:1 resonance,  $M_p$ , depends on the mass of the outer, more massive transiting planet  $M_t$  and its apparent eccentricity  $e$  as follows:

$$M_p = \frac{e}{\sqrt{3/2}} M_t \quad (1)$$

(Anglada-Escude et al. 2010). In this case  $M_p$  should be treated as an upper limit because it was obtained assuming circular orbits. The hypothetical inner, less massive planet is expected to produce perturbations which should be visible in TTV of WASP-3b.

To check if an inner perturber in the WASP-3 system may reproduce observed cyclic TTV, we generated 2232 synthetic  $O - C$  diagrams for orbits close to the 1:2 resonance. Following Rabus et al. (2009) we neglected the light-time effects and assumed that the planetary orbits are coplanar. We used the MERCURY package (Chambers 1999) and the Bulirsch-Stoer algorithm to integrate the equations of motion for this three-body problem. Parameters of the transiting planet and its host star were taken from Tripathi et al. (2010) and Pollacco et al. (2008), respectively. The initial circular orbits were assumed. The semi-major axis of the perturber  $a_p$  was between  $0.0185$  and  $0.0215 \text{ au}$  ( $\pm 0.0015$

**Table 3.** Outer-perturber solutions which reproduce the observed  $O - C$  variation.  $a_p$  denotes the semi-major axis of the perturbing planet,  $M_p$  is its mass,  $P_p$  is its orbital period,  $K_p$  is the expected semi-amplitude of the radial-velocity variation and  $\chi_{\text{red}}^2$  is the lowest value of reduced chi-square for direct model fitting.

$a_p$ (au)	$M_p$ ( $M_{\oplus}$ )	$P_p$ (d)	$K_p$ ( $\text{m s}^{-1}$ )	$\chi_{\text{red}}^2$
0.0441 – 0.0443	6 – 10	3.03 – 3.05	2.3 – 3.8	2.4
0.0493 – 0.0498	10	3.58 – 3.64	3.7	2.8
0.0506 – 0.0511	15	3.72 – 3.78	5.3	1.5

au away from the 2:1 resonance) in steps of 0.0001 au. The mass of the second planet  $M_p$  was varied from 5 to 30  $M_{\oplus}$  in steps of 5  $M_{\oplus}$ . The upper limit was calculated according to equation (1) assuming  $e = 0.05 \pm 0.04$ . The initial phase shift toward the transiting planet (in fact, an initial mean anomaly of the perturber),  $\phi$ , was between  $0^\circ$  and  $330^\circ$  in steps of  $30^\circ$ . Computations covered 640 periods of WASP-3b, i.e. the time span covered by observations. Synthetic  $O - C$  diagrams were searched for periodicity with the ANOVA method and the mean amplitude of variation was determined. The procedure was repeated for the 3:2 resonance.

Periodicity close to  $P_{\text{ttv}}$  was not found near either resonance. That allowed us to eliminate the scenario where the inner perturber generates the observed TTV signal.

#### 4.4 Outer perturber

Applying methods described in section 4.3, we generated 19680 synthetic  $O - C$  diagrams assuming the existence of an outer perturber in the system. Both planets were assumed to orbit the star in initial circular orbits. We investigated cases with the second planet close to 2:1, 3:1, 3:2, and 5:3 MMRs,  $\pm 0.0020$  au away from each resonance. The mass of the perturber  $M_p$  was varied from 5 to 50  $M_{\oplus}$  in steps of 5  $M_{\oplus}$ . Solutions close to observed cyclic TTV were studied in detail by varying  $M_p$  and  $\phi$  in steps  $\Delta M_p = 1 M_{\oplus}$  and  $\Delta \phi = 15^\circ$ , respectively.

We found a family of solutions close to 5:3 MMR recovering the period close to  $P_{\text{ttv}}$  for  $a_p$  between 0.0441 and 0.0443 au and  $M_p$  between 7 and 10  $M_{\oplus}$ . The exemplary synthetic  $O - C$  diagram is plotted in Fig. 4a. We also found 2 groups of solutions close to the 2:1 MMR. In the first one the perturber has  $M_p$  of 10  $M_{\oplus}$  and  $a_p$  between 0.0493 and 0.0498 au. Fig. 4b shows the shape of expected signal which, despite being periodic, clearly shows a deformation of the amplitude. The second group of solutions may be found for  $a_p$  between 0.0506 and 0.0511 au and  $M_p$  of 15  $M_{\oplus}$ . As it is shown in Fig. 4c, periodic variation may be modulated by a long-term periodicity significantly affecting the amplitude of variations. This long-term cyclic variability is caused by the resonant oscillations of the planetary orbits. Table 3 summarises parameters of proposed models.

No solutions close to observed TTV variation were found near resonances 3:1 nor 3:2. Orbits far away from MMRs were analysed using the PTMET code based on the perturbation theory (Nesvorný & Morbidelli 2008; Nesvorný 2009). A perturbing planet was put in initial circular or-

bits with semi-major axis  $a_p$  between 0.0370 and 0.1200 au in steps of 0.0002 au. As the amplitude of TTV signal was found to scale nearly linearly with the perturber’s mass (Nesvorný & Morbidelli 2008),  $M_p$  was fixed and set equal 50  $M_{\oplus}$ . An initial phase shift toward the transiting planet  $\phi$  was between  $0^\circ$  and  $315^\circ$  in steps  $\Delta \phi = 45^\circ$ . A total of 3320 systems were analysed but no configuration reproducing the observed variation was found.

To quantify the quality of solutions collected in Table 3, the synthetic  $O - C$  diagrams were directly fitted to data points. The chi-square test favours the third group of solutions where the smallest reduced  $\chi_{\text{red}}^2 = 1.5$  was obtained for  $a_p = 0.0507$ . This value is significantly smaller than  $\chi_{\text{red}}^2 = 3.9$  for a model without a perturbing planet. The  $O - C$  diagram with the best-fitting model is presented in Fig. 5 where the residuals are also plotted. The expected semi-amplitude of the radial velocity variation caused by the perturber is expected to be  $\sim 5 \text{ m s}^{-1}$  and thus undetectable in the published radial velocity measurements. The most probable model was found to be stable dynamically. A simulation was run for  $10^6$  yr and no significant changes in the eccentricities were detected. The eccentricities of transiting and perturbing planet were found to be below 0.005 and 0.033, respectively.

Such a WASP-3 system would not be completely unusual with two planets close to the 2:1 MMR (see e.g. Gliese 876 b and c, Marcy et al. 2001) but the first one with such close-in planets and the less massive planet being in an outer orbit. The origin of such a system would be interesting in a context of the large-scale orbital migration in young planetary systems. A Super-Earth (10  $M_{\oplus}$ ) is expected to be caught in a trap when it is very close to the edge of the wide gap opened in a disk by a Jupiter-mass gas giant. This trapping prevents the outer planet from being locked in the 2:1 MMR. If a planet increases its mass by accretion, it may be released from such a trap and form a resonant configuration (Podlowska & Szuszkiewicz 2009). This scenario cannot be rejected in the case of the outer perturber in the WASP-3 system because the nowadays planet might be a rocky remnant core of a planet which has greater mass in the past – a hot Jupiter whose gaseous envelope was completely evaporated due to the proximity to the host star (Jackson et al. 2010).

## 5 CONCLUSIONS

In this paper we show that transit timing of WASP-3b cannot be explained by a constant period of the exoplanet. We emphasise that this finding is based on only a few data points. However, one may put forward provisional hypothesis which assumes the existence of a perturber in the system. As a result of simplified 3-body simulations, two groups of configurations which reproduce the observed TTV were identified close to the outer 2:1 MMR and one group close to the 5:3 MMR. A model with the hypothetical second planet of the mass of  $\sim 15 M_{\oplus}$  and orbital semi-major axis of 0.0507 au was found to be most likely. In this scenario both planets stay in the stable orbital resonance with a period ratio of 2.02, i.e. very close to the 2:1 MMR.

The expected radial-velocity semi-amplitude of the hypothetical second planet would be much smaller than the

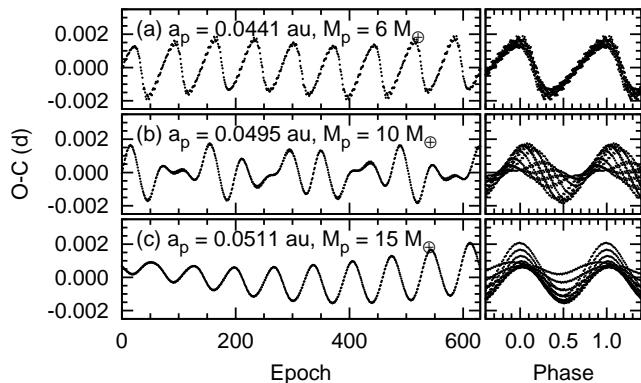


**Figure 4.** Examples of synthetic  $O-C$  diagrams which reproduce the observed variations, generated for an outer perturber. Left panels – the unfolded TTV signal, right panels – the TTV signal folded to period close to  $P_{\text{ttv}}$ .

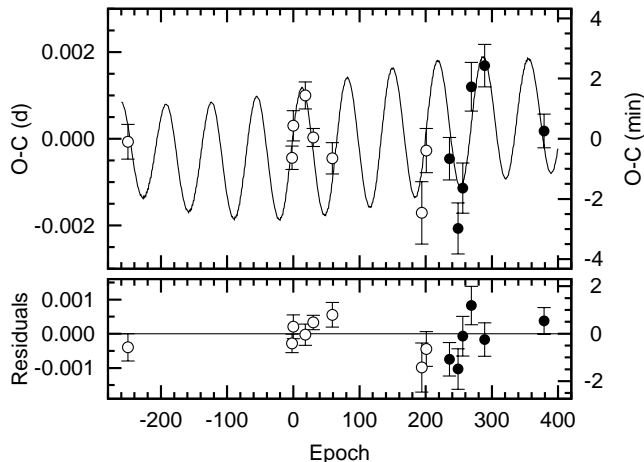


**Figure 5.** The  $O-C$  diagram with the best-fitting model which reproduces the observed variations. The mass of the perturber is  $15 M_{\oplus}$  and the semi-major axis of its initially circular orbit is  $0.0507$  au. Symbols are the same as in Fig. 2. Residuals are plotted in the bottom panel.

stellar jitter of WASP-3. This finding reduces chances of a direct detection of the perturber’s signal by further radial-velocity follow-ups. However, we showed that one cannot exclude the non-zero eccentricity of WASP-3b. Such an eccentric orbital solution may be an indirect fingerprint of the second planet in a wider orbit gravitationally pumping the eccentricity of the transiting planet.

Assuming the hypothetical second planet is also a transiting exoplanet, it would cause periodic flux drops of the host star. The depth of these transits would be in the range of 0.03–0.35 per cent (or 0.3–3.8 mmag) depending on the adopted mean planetary density – for a rocky planet (e.g. CoRoT-7b, Léger et al. 2009; Queloz et al. 2009) or an ultra-low-density hot Neptune (e.g. WASP-17b, Anderson et al. 2010), respectively. If one considers the mass of the hypothetical second planet and its proximity to the host star, the latter scenario seems to be less probable, causing transits to be shallow and difficult to detect.

As the TTV method requires many high-quality light curves, more data will be gathered for WASP-3b to confirm

or disprove the claimed variation in the  $O-C$  diagram. A long-time baseline of observations is needed to characterise possible resonant oscillations in the TTV signal. More accurate radial-velocity measurements are also required to gain deeper insight into orbital parameters of the transiting planet. Additionally, a transit of the predicted second planet could be observable with a large ground-based or space-based telescope.

## ACKNOWLEDGMENTS

GM and SR acknowledge support from the EU in the FP6 MC ToK project MTKD-CT-2006-042514. SR would also like to acknowledge support from DFG in program NE 515/32-1. DD acknowledges support from the project DO 02-362 of the Bulgarian Scientific Foundation. RN would like to acknowledge general support from DFG in programmes NE 515/23-1, 30-1 and 32-1. GM, RN and AN acknowledge support from the DAAD PPP/MNiSW project 50724260 *Eclipsing binaries in young clusters and planet transit time variations*. AN was also supported by the Polish Ministry of Science and Higher Education grant NN203 510938. CG and CM would like to thank the German National Science Foundation (DFG) for support in programs NE 515/30-1 and SCHR 665/7-1, respectively. M.Moualla would like to thank the Syrian government for their support. Part of this paper is a result of PAN/BAN exchange and joint research project *Spectral and photometric studies of variable stars*. This work has used Exoplanet Transit Database, <http://var.astro.cz/ETD>. We thank A.V. Krivov for helpful comments on an earlier version of the paper. Finally, we owe a debt of gratitude to the anonymous referee for constructive remarks and suggestions which improved the paper.

## REFERENCES

- Adams E.R., López-Morales M., Elliot J.L., Seager S., Osip D.J., 2010, *ApJ*, 714, 13
- Agol E., Steffen J., Sari R., Clarkson W., 2005, *MNRAS*, 359, 567
- Agol E., Steffen J., 2007, *MNRAS*, 374, 941
- Anderson D.R., Hellier C., Gillon M. et al. 2010, *ApJ*, 709, 159
- Anglada-Escude G., López-Morales M., Chambers J.E., 2010, *ApJ*, 709, 168
- Bean J.L., 2009, *A&A*, 506, 369
- Bean J.L., Seifahrt A., 2008, *A&A*, 487, 25
- Bessel M.S., 1990, *PASP*, 102, 1181
- Chambers J.E., 1999, *MNRAS*, 304, 793
- Díaz R.F., Rojo P., Melita M., Hoyer S., Minniti D., Mauas P.J.D., Ruž M.T., 2008, *ApJ*, 682, 49
- Everett M.E., Howell S.B., 2001, *PASP*, 113, 1428
- Fabrycky D.C., 2009, in Pont F., Sasselov D.D., Holman M.J., eds, *Proc. IAU Symp. 253, Transiting Planets*. Cambridge University Press, p. 173
- Ford E.B., Howell M.J., 2007, *ApJ*, 664, L51
- Gibson N.P., Pollacco D., Simpson E.K. et al., 2008, *A&A*, 492, 603
- Gibson N.P., Pollacco D., Simpson E.K. et al., 2009, *ApJ*, 700, 1078

- Gibson N.P., Pollacco D., Barros S. et al., 2010, MNRAS, 401, 1917
- Holman M.J., Murray N.W., 2005, Sci, 307, 1288
- Hrudková M., Skillen I., Benn C.R. et al., 2010, preprint (astro-ph/1001.0501)
- Jackson B., Barnes R., Raymond S.N., Fortney J., Greenberg R., 2010, BAAS, 41, 444
- Kipping D.M., 2009, MNRAS, 392, 181
- Lee J.W., Kim S.-L., Kim C.-H., Koch R.H., Lee C.-U., Kim H.-I., Park J.-H., 2009, AJ, 137, 3181
- Léger A., Rouan D., Schneider J. et al., 2009, A&A, 506, 287
- Mandel K., Agol E., 2002, ApJ, 580, 171
- Marcy G., Butler R., Fischer D., Vogt S., Lissauer J., Rivera E., 2001, ApJ, 556, 296
- Mardling R.A., 2007, MNRAS, 382, 1768
- Meschiari S., Wolf A.S., Rivera E., Laughlin G., Vogt S., Butler P., 2009, PASP, 121, 1016
- Miller-Ricci E., Rowe J.F., Sasselov D. et al., 2008a, ApJ, 682, 586
- Miller-Ricci E., Rowe J.F., Sasselov D. et al., 2008b, ApJ, 682, 593
- Miralda-Escudé J., 2002, ApJ, 564, 1019
- Mugrauer M., Berthold T., 2010, Astron. Notes, 331, 449
- Nesvorný D., Beaugé C., 2010, ApJ, 709, 44
- Nesvorný D., Morbidelli A., 2008, ApJ, 688, 636
- Nesvorný D., 2009, ApJ, 701, 1116
- Niedzielski A., Maciejewski G., Czart K., 2003, Acta Astronomica, 53, 281
- Poddaný S., Brát L., Pejcha O., 2010, New Astron., 15, 297
- Podlewska E., Szuszkiewicz E., 2009, MNRAS, 397, 1995
- Pollacco D., Skillen I., Collier Cameron A. et al., 2008, MNRAS, 385, 1576
- Qian S.-B., Liao W.-P., Zhu L.-Y., Dai Z.-B., Liu L., He J.-J., Zhao E.-G., Li L.-J., 2010, MNRAS, 401, 34
- Queloz D., Bouchy F., Moutou C. et al., 2009, A&A, 506, 303
- Rabus M., Deeg H.J., Alonso R., Belmonte J.A., Almenara J.M., 2009, A&A, 508, 1011
- Raetz St., Mugrauer M., Schmidt T.O.B. et al., 2009a, Astron. Notes, 330, 459
- Raetz St., Mugrauer M., Schmidt T.O.B. et al., 2009b, Astron. Notes, 330, 475
- Saar S.H., Butler R.P., Marcy G.W., 1998, ApJ, 498, L153
- Schwarzenberg-Czerny A., 1996, ApJ, 460, 107
- Silvotti R., Schuh S., Janulis R. et al., 2007, Nat, 449, 189
- Simon A., Szatmáry K., Szabó G.M., 2007, A&A, 470, 727
- Simpson E.K., Pollacco D., Hébrard G. et al., 2010, preprint (astro-ph/0912.3643)
- Southworth J., Hinse T.C., Jorgensen U.G. et al., 2009, MNRAS, 396, 1023
- Steffen J.H., Agol E., 2005, MNRAS, 364, 96
- Steffen J.H., Gaudi B.S., Ford E.B., Agol E., Holman M.J., 2007, preprint (astro-ph/0704.0632)
- Tripathi A., Winn J.N., Johnson J.A. et al., 2010, ApJ, 715, 421
- Van Hamme W., 1993, AJ, 106, 2096
- Zahn J.-P., 1977, A&A, 57, 283